Calculation of the Dancoff Factor in Pebble Bed Reactors using Empirical Chord Length Distributions

BSc. Thesis
Luuk Buijs

Supervisors:
ir. Gert Jan Auwerda
ir. Frank Wols

Delft University of Technology
Faculty of Applied Sciences
Department of Radiation, Radionuclides & Reactors
Section Physics of Nuclear Reactors

August 6, 2012

Abstract

The Dancoff factor is a key element investigating very high temperature reactors (VHTR), because of the nature of their fuel design. Because the fuel particles are located close to one another in the moderator background, neutrons are more likely to enter adjacent fuel lumps before colliding with the moderator (as opposed to conventional reactor fuel designs). Therefore the self-shielding effect of the fuel is increased and has a strong impact on the overall criticality of the reactor. Dancoff factors have been calculated in the past for these reactor desings, but efficient investigation requires fast and flexible methods for these calculations. Earlier research includes the application of the chord length method to the calculation of the Dancoff factor for VHTR fuel designs. This approach proved to be successful in determining the Dancoff factor to some extent, but more accurate chord length probability density functions (PDFs) are required for better results.

In this research, two Fortran codes are written in order to generate empirical PDFs. The first code generated a distribution of TRISO fuel particles and constructed the PDF for path lengths between those particles. The second code determined the PDF of chord lengths through the moderator between fuel zones in a pebble bed reactor. The PDFs that were generated proved to be a more accurate approximation than the distribution functions used in earlier research, mainly due to the incorporation of the dual-sphere model of the fuel design. Several PDFs for a variety of fuel zone packing fractions and pebble sizes were evaluated using a MATLAB script. This approach allowed for a separate investigation of different probabilities that contribute to the overall Dancoff factor of the system. The expected behavior of these probabilities was successfully demonstrated, and the overall Dancoff factors were calculated. Results from the analytical approach yielded an overestimation of the Dancoff factor, which could be partly corrected by using the emprical PDFs.

The separate calculation of the contributing probabilities allows for a very flexible method of determining the Dancoff factor. Any combination of packing fraction and pebble size can directly be evaluated once the two PDFs have been determined, be it analytically or empirically.

Contents

Chapter 1

Introduction

Following the disaster at the Fukushima Daichii nuclear plant in 2011, the public popularity of nuclear energy has rapidly decreased. Germany announced the shutdown of eight of its reactors and its intentions to close the rest by 2022. France started the process of revisiting their nuclear safety regulations and investigating the safety of their operational nuclear plants. Meanwhile, due to the rapidly increasing global energy consumption and the decrease in fossil fuel availability [1], the need for more reliable energy sources has been receiving increasing attention worldwide. Predictions for the upcoming decennia [2] and the pressing matter of global warming and climate change place even more emphasis on their development. The safety and environmental impact of these energy sources will be key factors in determining their success. Nuclear energy must face the same challenges in order to regain its popularity.

While older reactor designs are found not to meet current safety regulations, newly developed safer reactor designs are introduced. The upcoming decennium will see the implementation of Generation III+ reactor designs and the development of the Generation IV reactor types. The Generation IV initiative is an international cooperation aimed at facilitating the development of the new generation of nuclear reactors [3]. The main goals of the initiative include sustainability, safety, reliability and affordability. It consists of 6 new system designs, among which the Very-High-Temperature reactor (VHTR). The Pebble Bed Reactor (PBR) is a specific VHTR design that involves graphite pebbles filled with TRISO fuel particles.

1.1 The pebble bed reactor

The pebble bed reactor is a graphite-moderated VHTR, cooled by gaseous helium. The reactor vessel is filled with stacked graphite pebbles containing TRISO fuel particles and is lined with graphite reflectors (see Figure 1.1). This pebble bed allows for the helium coolant to flow through the space inbetween the pebbles, as well as through the reflectors.

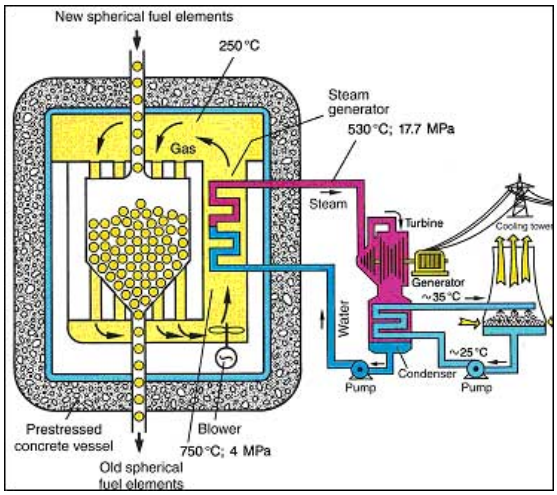

Figure 1.1: Schematic overview of a pebble bed reactor [4].

A standard pebble design consists of a 50mm diameter graphite sphere filled with randomly distributed TRISO fuel particles, and a 5mm thick fuel free graphite shell on the outside. The TRISO fuel particles consist of a uranium and thorium fuel kernel of up to 500μm in diameter coated with carbon layers of typically 200μm total thickness. For a schematic view of this type of pebble, see Figure 1.2. The pebbles can be continuously transported in and out of the vessel during operation of the reactor. This type of pebble is already in use in the HTR-10 at the Tsinghua University in China [5].

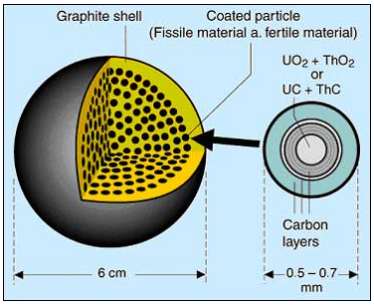

Figure 1.2: Schematic cross-section of a pebble [4].

One of the main advantages this brings as opposed to a conventional water-cooled reactor is that no internal piping is required to facilitate the coolant flow. Water-cooled systems are often very costly due to the cooling system complexity and extensive safety systems. Additionally, the water can become radioactive, causing the embrittlement of the high-pressure piping. A pebble-bed reactor cooled by helium contains no piping in the core and the coolant does

not contain hydrogen (helium is far less susceptible to radiation), ruling out the possibility of embrittlement. Another advantage is that the pebble bed reactor can operate at considerably higher temperatures than conventional systems. The helium exits the vessel at up to 1000 degrees Celsius, allowing for a highly efficient conversion to mechanical energy by gas turbines, and the generation of hydrogen as a byproduct.

However, the primary reason why the pebble bed reactor is so interesting, is that it can be designed to be passively safe. When the temperature in the reactor rises, negative feedback in the system will eventually cause the chain reaction to stop, mainly due to an effect called Doppler broadening. Additionally, the TRISO particle coating is designed to safely contain the fuel and reactants up to a temperature of 1600 degrees Celsius, which has been successfully tested in the HTR-10 [5].

1.2 The Dancoff factor

In a nuclear reactor, the neutrons released by fission have a kinetic energy that exceeds the thermal spectrum of most heavy nuclides used as fuel in a nuclear reactor. Moderator material is therefore used to slow down these neutrons through moderator collisions. When a neutron has suffered a sufficient number of moderator collisions its energy will be in the thermal range, resulting in a relatively high fission cross section. It can then induce a next fission reaction.

In a normal reactor geometry, the moderator and fuel are placed in separate regions. This is mainly because the neutrons, while they are slowed down, can become very susceptible to capture in absorption resonances of a nuclide such as uranium-238. In a pebble bed reactor however, the fuel lumps are located close to one another inside the moderator. Therefore, the probability that a neutron escapes a fuel lump and has its first interaction in the moderator, usually referred to as the first-flight escape probability, must be corrected for the chance that the neutron enters another fuel lump. This probability is called the Dancoff factor [6], and it is very important in calculating collision probabilities and resonance integrals.

The Dancoff factor can be conveniently split into two factors, the first of which is called the intra-Dancoff factor. This factor accounts for all the fuel lumps inside the same pebble. The second is called the inter-Dancoff factor and accounts for all the fuel lumps located inside the other pebbles. The Dancoff factor was first introduced by Dancoff and Ginsburg in 1944 [7]. Various methods have since been applied to compute it, both analytical [10][11] and by computer simulation [12][13]. Prior to the work of Dancoff and Ginsburg, Dirac used the chord length method to replace complicated integrals over angles and surfaces by simple one-dimensional integrals over chord length probability density functions (PDF), in order to calculate neutron multiplication factors for finite volumes. This approach can also be used to simplify Dancoff factor calculations, as was shown by Ji and Martin [6].

1.3 Research outline

As mentioned in the previous section, Dancoff factors have been calculated by means of Monte Carlo simulation, yielding excellent results. However, computation time has been prohibitive, especially if the simulations become too extensive. Analytical or semi-analytical methods have proven to be a quicker and far more flexible solution, but it is difficult to achieve accurate results because of the complexity of the geometry.

As suggested by Ji and Martin [6], the chord length method can be used to simplify analytical calculation of finite medium Dancoff factors. This method involves evaluation of integrals over chord length PDFs of the finite medium of interest. It has proven to be a flexible and accurate method, only limited by the precision of the used PDFs. Ji and Martin derived analytical approximations for these PDFs in previous work [14], but empirical generation of these PDFs can prove to be more accurate. The primary aim of this research is to improve the accuracy of the model by Ji and Martin by implementing empirical PDFs.

A new Fortran code, MC-PDF-LB is written to generate empirical chord length PDFs of different TRISO configurations in an infinite medium. These PDFs are used to calculate the intra-Dancoff factor by means of the analytical method proposed by Ji and Martin. The results are compared to those calculated using the original approximations of the PDFs, and to Dancoff factors calculated by a benchmark Monte Carlo simulation. Additionally, the code PDF-PB is used to generate chord length PDFs of different pebble bed geometries. Evaluation of these PDFs combined with the PDFs from MC-PDF-PB yields the inter-Dancoff factors, which is compared to factors calculated using the original approximations of the PDFs.

Chapter 2 will cover the basic theory of nuclear reactor physics, followed by a derivation of the analytical formala by Ji and Martin. Chapter 3 is a detailed description of the two codes used to generate the PDFs, PDF-PE and PDF-PB, including uncertainty analysis. Chapter 4 will cover the results produced by the codes and numerical evaluation of the PDFs, accompanied by their discussion. Conclusions drawn from the results and recommendations for future research are summarized in Chapter 5.

Chapter 2

Theory

In this chapter, the basics of nuclear reactor physics relevant to study of the Dancoff factor are explained, followed by a short description of the Dancoff factor itself. Next, a derivation of the chord length method as described by Ji and Martin is given.

2.1 Nuclear reactor physics

This section will give a brief explanation of the basic concepts in nuclear reactor physics that are relevant to the study of the Dancoff factor.

2.1.1 Cross sections

The probability that a neutron has a certain interaction with a target nucleus is determined by the relevant nuclear cross section. For a single nucleus or thin layer of nuclei, the microscopic cross section is defined:

$$\sigma = \frac{\text{number of interactions/nucleus/s}}{\text{number of incident neutrons/cm}^2\text{/s}} \tag{2.1}$$

The value of the relevant cross section depends mainly on the type of interaction, the energy of the incident neutron, and the type of the target nucleus. The two primary forms of interaction are absorption (σ_A) and scattering (σ_S). These two cross sections can be further subdivided into partial cross sections that govern the subsequent event. For example, absorption may lead to fission (σ_f) or gamma radiation (σ_γ). While studying the Dancoff factor, it is often more convenient to look at the total microscopic cross section σ_T, which is independant of the type of interaction. Because the individual cross sections are essentially probabilities, they can be added up:

$$\sigma_T = \sigma_A + \sigma_S = \sigma_f + \sigma_\gamma + ... \tag{2.2}$$

In a nuclear reactor system, incident neutrons face a complete lattice of nuclei. The macroscopic cross section determines the probability of interaction with all the nuclei combined and is given by:

$$\Sigma_T = N\sigma_T, \tag{2.3}$$

where the number N is the density of nuclei. As will be explained in subsequent sections, the Dancoff factor can be determined by evaluation of the probability that a neutron reaches another fuel lump without having an interaction with a nucleus. The probability that a neutron travels a distance x through the medium without an interaction is given by:

$$P(\text{no interaction}) = e^{-\Sigma_T x}. \tag{2.4}$$

2.1.2 Resonance shielding

In order to successfully operate a nuclear reactor, neutrons released by fission must engage in subsequent reactions. Because the energy of the neutrons released by fission generally exceeds that required for a sufficiently high fission cross section (<0.01 eV), the neutrons must be slowed down by suffering moderator collisions. Due to a large absorption cross section for thermal neutrons in fuel, the flux of thermal neutrons drops rapidly over distance in a fuel lump. This means that the outer regions of the fuel are 'shielding' the inner regions, an effect that is therefore referred to as the self-shielding of the fuel. Additionally, while the neutrons are being slowed down to thermal range, their energies will often match those of a number of capture resonances. These are large peaks in the absorption cross section spectrum of heavy nuclides such as uranium-238 and thorium-232 (see Figure 2.1).

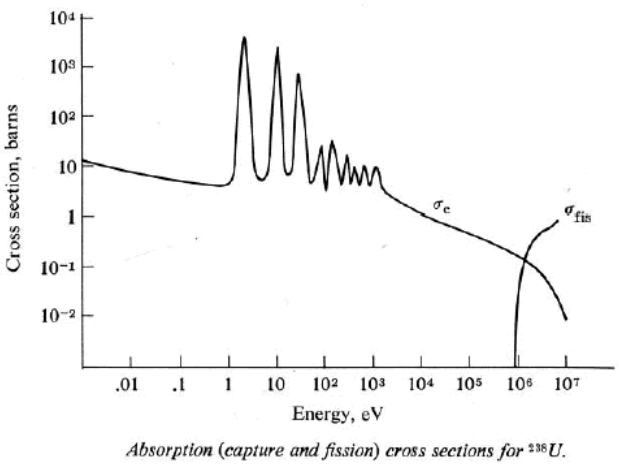

Figure 2.1: Neutron absorption spectrum of uranium-238 [15].

The neutron flux will be extremely low for the energies of those capture resonances due to the increased self-shielding of the fuel. This must be taken into account when calculating total neutron flux, which is usually done using group-wise cross sections. The Dancoff factor, which will discussed in the following sections, plays an important role in these calculations.

2.1.3 Criticality

The concept of reactor criticality is not essential in this specific study of the Dancoff factor. However, because it is a key factor in the operation of nuclear reactors and it is strongly influenced by the Dancoff factor in the case of pebble bed reactors [13], it is still very relevant. Because successful operation of a nuclear reactor requires a self-sustaining chain reaction, the number of neutrons in each reaction generation is important. The multiplication factor is therefore defined as:

$$k_{eff} = \frac{\text{number of neutrons in given generation}}{\text{number of neutrons in preceding generation}}. \tag{2.5}$$

This factor gives information concerning the criticality of the reactor. In the case that k_{eff} equals 1, the reaction is self-sustaining and the reactor is called critical. Because in this situation the amount of energy produced is constant this situation implies a safe and effective operation of the reactor. While the reactor is being started, k_{eff} is slightly higher than 1 and the reactor is called supercritical. Contrary, when k_{eff} is smaller than 1, the number of fission reaction per unit time is decreasing and the reactor is called subcritical. This is the case when the reactor is being shut down.

2.2 The Dancoff factor

As explained in the previous sections, in order for a fast neutron to be slowed down into thermal range, it must suffer moderator collisions. The probability that a neutron excapes a fuel lump and has its next interaction in the moderator is essential in governing this process. This probability P_M is equal to the first flight probability P_{esc}, which denotes the probability that a neutron escapes the fuel lump.

In a pebble bed reactor however, the fuel lumps are located at smaller distances to one another inside the moderator. Therefore, the neighbouring fuel lumps must be taken into account when determining P_M. This influence can be described by the Dancoff factor C, the probability that a neutron will enter another fuel lump inside the same pebble or in another pebble. P_M now becomes:

$$P_M = P_{esc}\frac{1-C}{1-C(1-P_F)}. \tag{2.6}$$

Here P_F denotes the probability that a neutron suffers an interaction inside an encountered fuel kernel. From the equation it can be seen that a higher Dancoff factor implies a lower P_M, which is often referred to as the "shadowing effect". For simplification, it is evaluated only for neutron energies of 10-100 eV because most of the capture resonances of uranium-238 are in this range, and because the graphite total cross-section only varies slightly in this range.

2.3 Application of the chord length method

This section will cover some of the derivations done by Ji and Martin in applying the chord length method to the calculation of the Dancoff factor.

First, consider the generalized case where arbitrary nonreentrant shapes are dispersed randomly in a background moderator. The fission neutrons generated in the fuel lumps may be slowed down in the moderator and enter the resonance energy range of the absorption spectrum and be absorbed inside the fuel lump. In order to model this, a uniform and isotropic source of resonance energy neutrons is assumed in the moderator. For a source density Q neutrons/cm^3·s at a point r' in the moderator, the rate at which neutrons enter a fuel lump through a small surface element dA at surface point r can written as [6]:

$$J = \frac{Q\lambda A}{4}\left[1 - \frac{\int dA \int d\Omega \cos\theta (e^{-l/\lambda})}{\int dA \int d\Omega \cos\theta}\right]. \tag{2.7}$$

Here θ is the angle between $r - r'$ and dA, l is the length of the chord through the point r in the direction (θ, ϕ) to the surface of any other fuel lump that can see the fuel lump of interest. $d\Omega$ is a solid angle element in that same direction and A is the total surface area of the finite volume. λ is the mean free path length of resonance neutrons through the moderator, defined by the macroscopic cross section Σ_T. This equation was found by Dancoff and Ginsburg [7]. The first part of the equation is the total rate at which resonance neutrons would enter a fuel lump, if that fuel lump would be the only one that existed. The second part is the reduction in that rate due to neighbouring fuel lumps, of which the term in brackets is called the Dancoff factor C.

Introducing the PDF for the distribution of chord lengths between fuel lumps in the moderator, this equation can be simplified. According to Dirac [8], the chord length distribution PDF $f(l)$ is defined such that for any function $g(l)$:

$$\int f(l)g(l)dl = \frac{\int dA \int d\Omega \cos\theta [g(l)]}{\int dA \int d\Omega \cos\theta}, \tag{2.8}$$

So that the infinite medium Dancoff factor becomes:

$$C_\infty = \int f(l)e^{-l/\lambda}dl. \tag{2.9}$$

This equation reduces the calculation of an infinite medium Dancoff factor to the determination of the chord length PDF between fuel lumps in the moderator,

an approach that can be easily applied to TRISO fuel particles. In order to calculate Dancoff factors for pebble bed reactors however, the finite geometries of the pebbles must be taken into account. The intra-Dancoff factor C_{intra} accounts for the fuel lumps inside the same finite medium (e.g. pebble), and the inter-Dancoff factor C_{inter} accounts for all the fuel lumps in other finite media.

2.3.1 Intra-Dancoff factor

Following the same method for a finite medium, the average intra-Dancoff factor over all fuel lumps can be written as:

$$C_{intra} = \frac{1}{4\pi V} \int dA \int d\Omega \cos\theta \int_{\text{min\_d}}^{L} C(l) dl, \tag{2.10}$$

where V is the total volume and A the total surface area of the finite medium. L is the maximum distance to the boundary of the finite medium, and min_d is the minimum distance between fuel lumps, for example due to the coating radius of the TRISO particles. This equation allows for a similar approach as in Equation 2.8, again using the chord length PDF. After a number of algebraic manipulations, this leads to:

$$C_{intra} = \frac{1}{\langle L \rangle} \int dL F(L) \int_{\text{min\_d}}^{L} dl \int_{\text{min\_d}}^{l} dl' f(l') e^{-l'/\lambda}, \tag{2.11}$$

Where $\langle L \rangle = 4V/A$ is the mean chord length for the finite medium, and $F(L)$ the PDF for the distribution of chord lengths inside the finite medium. The multidimensional integrals over surface and angle domains has been reduced to the evaluation of one-dimensional integrals over two chord length PDFs. Equation 2.11 is used to evaluate the empirical PDFs generated in Chapter 3. For the case of a pebble with fuel zone radius R_1 filled with TRISO fuel particles, $F(L)$ is well known, and $f(l)$ was approximated by Ji and Martin [14] using the single-sphere model (see Figure 2.2):

$$F(L) = \frac{L}{2R_1^2}, \qquad 0 < L < 2R_1; \tag{2.12}$$

$$f(l) = \frac{1}{\langle l \rangle} e^{-l/\langle l \rangle}, \qquad 0 < l < \infty, \tag{2.13}$$

where

$$\langle l \rangle = \frac{4r}{3} \frac{1 - frac'}{frac'}$$

is the mean chord length between two fuel kernels and $frac'$ the ratio of total fuel kernel volume to the whole medium volume. Note that $frac' = frac \cdot (r/R)^3$, with $frac$ the ratio of total of TRISO particle volume to the

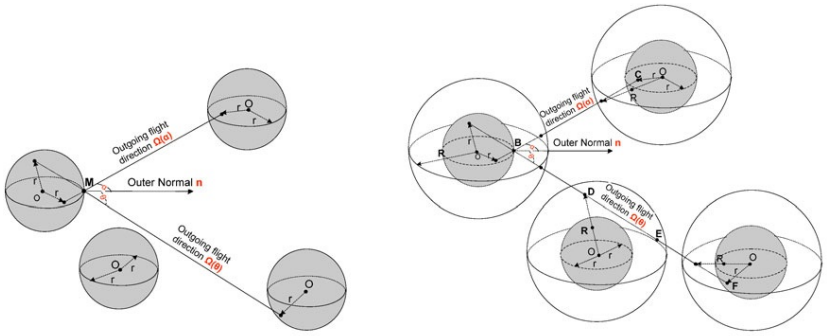

Figure 2.2: Single-sphere (left) and dual-sphere (right) models of TRISO fuel particles [6]

.

whole medium volume, also known als the "volume packing fraction". The average intra-Dancoff factor is now defined as:

$$C_{intra} = C_\infty \left[1 - P^*_{esc}\right], \tag{2.14}$$

Here the infinite medium Dancoff factor and the first flight escape probability are given by:

$$C_\infty = \frac{\lambda^*}{\langle l \rangle}, \tag{2.15}$$

$$P^*_{esc} = \frac{3}{4}\left(\frac{\lambda^*}{R_1}\right) - \frac{3}{4}\left(\frac{\lambda^*}{R_1}\right)^2 e^{-2(R_1/\lambda^*)} + \frac{3}{8}\left(\frac{\lambda^*}{R_1}\right)^3 \left[1 - e^{-2(R_1/\lambda^*)}\right], \tag{2.16}$$

with

$$\Sigma^* = \frac{1}{\lambda^*} = \frac{1}{\lambda} + \frac{1}{\langle l \rangle} \tag{2.17}$$

the effective cross section of the finite medium. This model yielded fairly accurate results [6], except for a small underestimate of the intra-Dancoff factor at lower packing fractions. Although the deviation was well in the acceptable range, a dual-sphere model might accomplish a better approximation.

2.3.2 Inter-Dancoff factor

The inter-Dancoff factor can be defined as the probability that a neutron escaping from a fuel lump in a finite volume enters another fuel lump in a different finite volume. It can be expressed as a function of several basic probabilities:

$$C_{inter} = P_1 P_2 P_3 \frac{1}{1 - P_2 P_{tr}}, \tag{2.18}$$

with:

- P_1 the average probability that a neutron escaping a fuel lump in a finite volume escapes the volume without entering another fuel lump or colliding with the moderator, equivalent to P_{esc}^*;
- P_2 the average probability that a neutron escaping from a finite volume enters another volume without colliding with the moderator;
- P_3 the average probability that a neutron incident on a finite volume enters a fuel lump within that volume;
- P_{tr} the average probability that a neutron incident on a finite volume traverses it without entering any fuel lump or colliding with the moderator.

Through application of the chord length method, these probabilities can be derived:

$$P_1 = \frac{1}{\langle L \rangle} \int dLF(L) \int_{\text{min\_d}}^{L} dl e^{-l/\lambda} \left(1 - \int_{\text{min\_d}}^{L} f(l')dl'\right), \tag{2.19}$$

$$P_2 = \int H(S) e^{-S/\lambda}, \tag{2.20}$$

$$P_3 = \int dLF(L) \int_{\text{min\_d}}^{L} f(l) e^{-l/\lambda} dl, \tag{2.21}$$

$$P_{tr} = \int dLF(L) e^{-L/\lambda} \left(1 - \int_{\text{min\_d}}^{L} f(l')dl'\right). \tag{2.22}$$

$H(S)$ is the chord length PDF between two volumes in an infinite background medium of volumes. This PDF can be interpreted as the distribution of chord lengths through the moderator between two pebbles in the case of a pebble bed. Ji and Martin approximated $H(S)$ by means of an exponential PDF:

$$H(S) = \frac{1}{\langle S \rangle} e^{-S/\langle S \rangle}, 0 < S < \infty, \tag{2.23}$$

with

$$\langle S \rangle = \frac{4R_1(1 - FRAC)}{3FRAC},$$

where $FRAC$ is the volume packing fraction of the pebble fuel zone in the whole medium. With this exponential PDF and the PDFs $f(l)$ and $F(L)$ as defined before, the separate probabilities are found to be:

$$P_1 = P^*_{esc}, \tag{2.24}$$

$$P_2 = \frac{1}{1 + \langle S \rangle / \lambda}, \tag{2.25}$$

$$P_3 = C_\infty \frac{\langle L \rangle}{\lambda^*} P^*_{esc}, \tag{2.26}$$

$$P_{tr} = 1 - \frac{\langle L \rangle}{\lambda^*} P^*_{esc}, \tag{2.27}$$

with C_∞ and P^*_{esc} as defined in Equations 2.15 and 2.16. The approximation made in Equation 2.23 yielded very poor results for P_2. In the next chapter, two Fortran codes are described that empirically determine $f(l)$ and $H(S)$ from TRISO distributions and a pebble stacking. By means of Equations 2.19 - 2.22, they can be evaluated to calculate inter- and intra-Dancoff factors.

Chapter 3

Fortran codes

This chapter covers the two Fortran codes written in order to obtain empirical chord length PDFs in TRISO distributions and pebble bed configurations. PDF-LB generates a random TRISO distribution and generates a chord length PDF by evaluating randomized neutron paths. PDF-PB loads a pregenerated pebble bed configuration, and generates a second chord length PDF by sampling the distance traveled through the moderator in a similar fashion. The PDFs are then evaluated by using a MATLAB script, and compared to the analytical results from Ji and Martin. In addition, a Monte Carlo benchmark simulation is used for comparison of the intra-Dancoff factor. Uncertainty calculations and the influence of packing fraction fluctuations are also discussed.

3.1 PDF-LB

The code used to generate TRISO distributions and their chord length PDFs consists of three parts. First the desired TRISO distribution is randomized, following a procedure similar to that of Ji and Martin [14]. Then the hypothetical neutron flight paths are simulated and their chord lengths sampled. The sampled chord lengths are used to generate the PDFs by using a histogram algorithm. Computation time for this code for 1 million neutrons is between roughly 4 hours and 18 hours depending on the packing fraction. Multiple PDFs can be generated for a single TRISO distribution.

3.1.1 Generating the TRISO distribution

The chord length PDF for distances between fuel lumps in the moderator should approximate that of an infinite distribution. To accomplish this, the fuel lumps are placed randomly inside a large cubical box. The box dimensions depend on the fuel zone radius of the pebbles to be studied. For example, the pebbles of interest in this research have a fuel zone radius of 25mm. That means that the maximum distrance traveled through the pebble is roughly 50mm. The neutrons

that are generated in this simulation must therefore not be able to reach the edge of the box within 50mm of their original position in order to generate a correct representation of the PDF.

The TRISO distribution is generated by randomizing single TRISO coordinates, and then checking for overlap with all TRISOs that were previously placed. If the TRISO overlaps with any of the other TRISOs, the coordinates are rejected and randomized again. This process is repeated until all the TRISO coordinates are accepted. The number of TRISO coordinates rejected increases as more TRISOs are generated, and therefore it strongly depends on the packing fraction of the desired distribution, given by:

$$frac = N_{TRISO} \frac{4\pi}{3} \left(\frac{R_{TRISO}}{L_{box}} \right)^3, \tag{3.1}$$

where R_{kernel} is the fuel kernel radius, R_{TRISO} the TRISO shell outer radius and L_{box} the cubical box edge length. This algorithm has been shown [16] to work well for packing fractions up to 32%. The packing fractions in this research range from 2% to 24%, which is far below the maximum achievable 62%, but well suited for studying practical situations.

3.1.2 Neutron path simulation

Once the TRISO distribution is generated, the individual neutrons are simulated. Note that the only relevant quantity obtained from the simulation is the flight path length through the moderator (ignoring moderator collisions) to a subsequent TRISO fuel kernel. This is a significant difference as opposed to standard Monte Carlo simulation of a neutron flight path.

First a random TRISO is chosen from the TRISO distribution. This TRISO must be located inside a predefined inner box centered at the center of the outer box. The dimensions of the inner box are chosen so that neutrons generated inside this box would need to travel at least the maximum distance to reach the edge of the outer box. In the case of a maximum travel distance of 50mm, the inner box surface must be at least 50mm away from the outer box surface. A summary of the input parameters used is given in Table 3.1. The TRISO dimensions used in this research are conform the NGNP Point Design [18], for easy comparison to the results by Ji and Martin.

Input parameter	Value
R_{kernel}	175μm
R_{TRISO}	390μm
L_{box}	110mm
L_{inner}	10mm
Σ_M	0.041mm^{-1}
$\Sigma_{coating}$	0.041mm^{-1}

Table 3.1: TRISO distribution related input parameters.

When the fuel kernel has been selected, the neutron direction is randomized as a cosine distributed angle. Then the neutron location inside the fuel kernel is generated by randomly selecting a location inside a cube with edges twice the kernel radius, and then checking if the neutron is inside the kernel itself. This has proven to be a far more efficient method than randomizing the neutron location inside the kernel right away by using for example spherical coordinates. The distance to the fuel kernel surface is calculated, and the neutron is moved to the surface intersection along its predetermined direction. Note that form this point on, the neutron travels through the TRISO coating and the moderator, and the distance traveled must be sampled.

As can be seen in Table 3.1, the moderator and TRISO coating are assumed to have the same total cross section. The cross sections of graphite moderator and the carbon coating are almost the same, so this is a valid approximation. This means that the distances traveled through these materials do not require separate registration. A quadratic formula is now used to determine whether or not the neutron path has an intersection with each of the other fuel kernels. If so, the distance to that intersection is registered and the smallest of these distances is sampled as the chord length. Whenever a neutron path does not cross another kernel, or the distance exceeds the maximum travel distance, no path length is sampled. These neutrons still contribute to the total neutron count however, which is important for normalization of the PDF and uncertainty calculations.

3.1.3 Chord length PDF

When all neutrons have been generated, a simple histogram algorithm is used to generate the PDF. The number of bins in the PDF depends on the number of neutrons generated: $N_{bin} = \sqrt{N_{neutron}}$. For every path length, the algorithm loops through all the bins to find the appropriate one. The PDF array will eventually contain a number of variables, which are shown in table 3.2.

Parameter	Meaning
d_{bin}	bin size [mm]
$\bar{L}$	average bin path length [mm]
N	bin count [-]
$\bar{N}$	normalized bin count [-]
u_N	bin count uncertainty [-]
$u_{\bar{N}}$	normalized bin count uncertainty [-]

Table 3.2: PDF array parameters.

The normalized bin count will be used as a representation for the actual PDF value $f(l)$, and is given by:

$$\bar{N} = \frac{N}{N_{neutron} d_{bin}}. \tag{3.2}$$

The standard count uncertainty for a Monte Carlo simulation is the square

root of the count divided by the number of experiments. Therefore the bin count uncertainty is:

$$u_N = \frac{\sqrt{N}}{N_{neutron}}, \tag{3.3}$$

so that

$$u_{\bar{N}} = \frac{\sqrt{N}}{N_{neutron}(x_2 - x_1)}. \tag{3.4}$$

The normalized bin count uncertainty is used in the calculations of Subsection 3.3.2 in order to determine the uncertainty in the Dancoff factor.

3.2 PDF-PB

The code used to determine the distribution of chord lengths between pebbles is organized in a similar fashion. First coordinates of a pregenerated pebble stacking are loaded. Then the neutron flight paths are simulated, and the path lengths are sampled. This process is described in the following subsections. A short analysis of the influence of packing fraction fluctuations near the reactor wall is also included. The construction of the PDF is identical to that in Subsection 3.1.3, and is therefore not discussed here. Computation time for 1 million neutrons was a little over 1 hour. Note that this excludes generating the pebble distribution, because only one distribution is required.

3.2.1 Pebble bed stacking

This program is capable of loading a pregenerated pebble stacking. The pebble stacking used in this research is a cylindrical bed generated using the expanding system method by Auwerda et al. [19]. The characteristics of this stacking and the pebbles are presented in Table 3.3. Note that the pebble fuel zone radius does not influence the pebble stacking geometry. The size of the pebbles can be adjusted by multiplying their coordinates with a scaling factor. Of course, other geometry parameters must be changed as well then.

Quantity	Value
N_{pebble}	67500
R_{bed}	150cm
R_{pebble}	30mm
R_{fuel}	25mm

Table 3.3: Pebble bed characteristics

3.2.2 Neutron path simulation

Once the pebble coordinates are loaded, single neutrons are generated. First the neutron direction is randomized, and a random location inside a cube of side twice the pebble fuel zone radius is selected. If the location is inside the actual fuel zone, it is accepted as the initial neutron location. The neutron is moved to the intersection with the fuel zone surface in the given direction. Then, the distance to the pebble outer radius is calculated and the neutron is moved to the pebble outer surface in the same direction. For all other pebbles, the program determines whether or not there is a surface intersection, and the one at the smallest distance from the neutron is selected. If the neutron would hit the pebble fuel zone, the distance to that fuel zone is sampled and the next neutron is generated. Otherwise, the neutron is placed on the other end of its trajectory through the pebble. The distance through the pebble is sampled and the process is repeated. Only the distances traveled through the pebble moderator regions are sampled. If a neutron does not hit any pebble, no distance is sampled. The 'leaked' neutrons are however counted among the total number of neutrons. When the desired number of neutrons has been sampled, the PDF array is constructed as shown in Table 3.2.

3.2.3 Neutron leakage

The Dancoff factor is most usefully applied when it is made independant of geometry. To this end, the pebble stacking must resemble an infinite medium of pebbles, and neutron leakage must be minimized. Additionally, pebble bed stackings show significant packing fraction fluctuations near the reactor wall [17]. Neutrons may therefore only be generated in pebbles at a minimum distance from the outer edges, to minimize leakage to the outer region or out of the pebble bed. This results in an inner cylinder at distance D_{out} from the outer surface. The number of leaked neutrons N_{leaked} is a good indication of the leakage to the outer region. Table 3.4 shows the leakage for a number of test runs at different pebble sizes for $D_{out} = 500$mm. From the table it is evident that $D_{out} = 500$mm is sufficient for smaller pebbles. For larger pebbles D_{out} is increased to 800mm.

R_{pebble}/R_{fuel}	% leaked
1.2	0.0002%
1.4	0.1555%
1.6	1.7027%
1.8	1.6388%
2.0	1.6140%
2.2	1.5825%
2.4	1.5691%

Table 3.4: Neutron leakage at $D_{out} = 500$mm

3.3 PDF processing

A MATLAB script is written in order to process the generated PDFs. The script numerically evaluates integrals over the PDFs in order to calculate the Dancoff factors and their uncertainty.

3.3.1 Dancoff factor calculation

Once the required PDFs are loaded into MATLAB, the script numerically evaluates the integrals described in Equations 2.11 and 2.19 - 2.22 in order to calculate the intra- and inter-Dancoff factors. The integrals are calculated as combinations of Riemann sums by a number of for loops. The average chord lengths $\bar{L}$ represent l, l', L and S. The integration steps dl, dl', dL and dS are represented by d_{bin} and the normalized bin counts $\bar{N}$ represent the values of $f(l)$ and $H(S)$. The limits of integration are given by the TRISO coating thickness $d_{coating}$ for d_min and the pebble fuel zone diameter for L_{max}. The intra-Dancoff factor for example is then given by:

$$C_{intra} = \frac{3}{4R_{fuel}} \sum_{i=1}^{N_{bin}} d_{bin} \frac{\bar{L}(i)}{2R_{fuel}} \sum_{j=1}^{i} d_{bin} \sum_{k=1}^{j} d_{bin} \bar{N}(k) e^{-\bar{L}(k)/\lambda}. \tag{3.5}$$

3.3.2 Uncertainty analysis

In order to calculate the Dancoff factor uncertainty, the individual normalized bin uncertainty $u_{\bar{N}}$ must also be processed. Because the integrals are evaluated as a combination of Riemann sums, the prefactors in these sums must accompany those bin uncertainties. This means that all the prefactors that an individual bin is multiplied with, must be quadratically added in order to obtain the total bin uncertainty prefactor. An example would be:

$$\Sigma = a_1 b_1 \bar{N}_1 + a_1 b_2 \bar{N}_1 + ..., \tag{3.6}$$

so that

$$u(\Sigma) = \sqrt{(a_1 b_1)^2 + (a_1 b_2)^2} \cdot u(\bar{N}_1) + ... \tag{3.7}$$

This same approach can be applied to calculate the uncertainties in the probabilities from Equations 2.19 - 2.22. The inter-Dancoff factor is a multiplication of these uncertainties. That means that the uncertainty in the inter-Dancoff factor is given by:

$$u(C_{inter}) = \sqrt{\left(\frac{dC_{inter}}{dP_1}\right)^2 u(P_1)^2 + \left(\frac{dC_{inter}}{dP_2}\right)^2 u(P_2)^2 + ...} \tag{3.8}$$

3.4 Benchmark

As a comparison for the method used to calculate the intra-Dancoff factor, a Monte Carlo benchmark simulation is created. This simulation operates in a similar fashion as PDF-LB, except that the TRISO particles are now created inside a single pebble fuel zone. The chord lengths that are sampled can directly be evaluated to produce the intra-Dancoff factor through:

$$C_{intra,B} = \frac{\sum e^{-l/\lambda}}{N_{neutron}}. \tag{3.9}$$

This is a very convenient and accurate method for determining the intra-Dancoff factor. Its computation time is significantly lower than that of PDF-LB, because far less TRISOs are created inside a single fuel zone as opposed to the large box from PDF-LB. However, it can not be used to generate usable chord length PDFs, because in order to do that there must be a uniform distribution of TRISOs for every path length up to the maximum path length. The PDFs generated from a single fuel zone are therefore not suited for calculation of the inter-Dancoff factor.

Chapter 4

Results and discussion

This chapter will present the results produced by the Fortran codes in Chapter 3, followed by the calculated Dancoff factors. The results for the intra-Dancof factor are compared to the analytical results and the results by the benchmark simulation, for several different packing fractions. The intra-Dancoff factor is compared to the analytical results as well as results from Spoor [16], both for different packing fractions and pebble sizes.

4.1 Intra-Dancoff factor

The intra-Dancoff factor was calculated by numerically evaluating the integrals from Equation 2.11 over the PDFs generated by the PDF-LB code. As mentioned in Chapter 2, the analytical description of the Dancoff factor by Ji and Martin uses a single sphere model [14] approximation shown in Equation 2.13. The influence of this model on the chord length distribution can be studied by comparison of that function to the PDFs generated by PDF-LB. The plot in Figure 4.1 is given as an example.

Because the dual-sphere model was used to generate the PDF with PDF-LB, that PDF shows no hit count for chord lengths under L =0.215mm, which is the total thickness of the coating. The approximation by Ji and Martin on the other hand, does show hit count in that region, because the single-sphere model allows for overlap of the TRISO coating. This should lead to a slight overestimate of the Dancoff factor by the analytical approach, because neutrons are less likely to have an interaction with the moderator before entering a fuel kernel at these smaller path lengths. The influence of this effect should increase with TRISO packing fraction, resulting in a higher hit count for smaller chord lengths.

The results for the intra-Dancoff factor are presented in comparison to the analytical results from Equation 2.14, and the Monte Carlo benchmark simulation in Table 4.1. Both PDF-LB and the benchmark simulation were performed for 1 million neutrons.

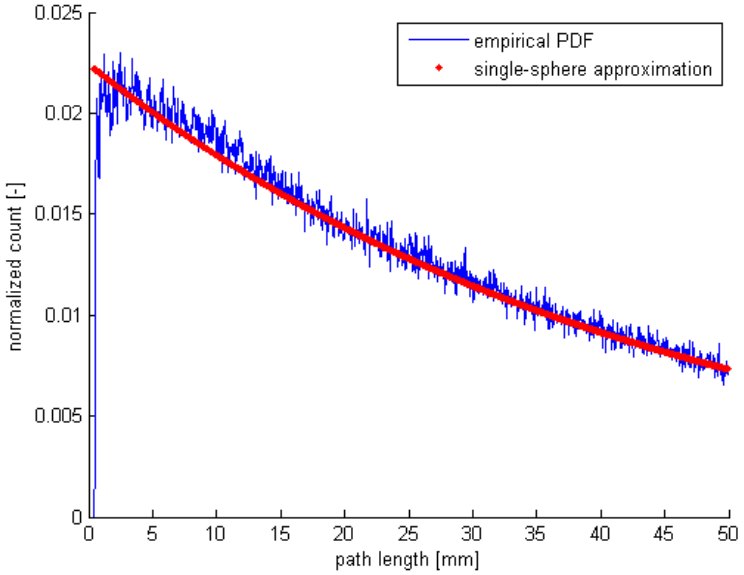

Figure 4.1: Comparison of empirical PDF to analytical approximation of the TRISO PDF $f(l)$

.

Packing fraction	$C_{intra,PDF}$	$C_{intra,MC}$	$C_{intra,A}$
0.04	0.15332 ± 0.00029	0.15532 ± 0.00039	0.15742
0.08	0.27214 ± 0.00040	0.27410 ± 0.00052	0.27693
0.12	0.36568 ± 0.00048	0.36598 ± 0.00060	0.36971
0.16	0.43170 ± 0.00053	0.43865 ± 0.00066	0.44323
0.20	0.49387 ± 0.00057	0.49664 ± 0.00070	0.50259
0.24	0.54226 ± 0.00061	0.54650 ± 0.00073	0.55132

Table 4.1: Intra Dancoff factor for various packing fractions. PDF = results from PDF-LB, MC = Monte Carlo Benchmark, A = analytical results.

Results from the evaluation of the PDFs are in reasonable agreement with the benchmark calculation, with errors ranging between 0.1% and 2.5% and an average error of 0.8%. These errors exceed the uncertainty range, so the accuracy of the method is not perfect. The aforementioned prediction concerning the overestimation by the single-sphere model seems to be supported by the results in Table 4.1, which show a small overestimation (average error 1.2%) of the Dancoff factor by the analytical formula that increases with TRISO packing fraction. Figure 4.2 shows a plot of these results from which the deviation is evident.

This error appears to be fixed when evaluating the PDFs from PDF-LB (see

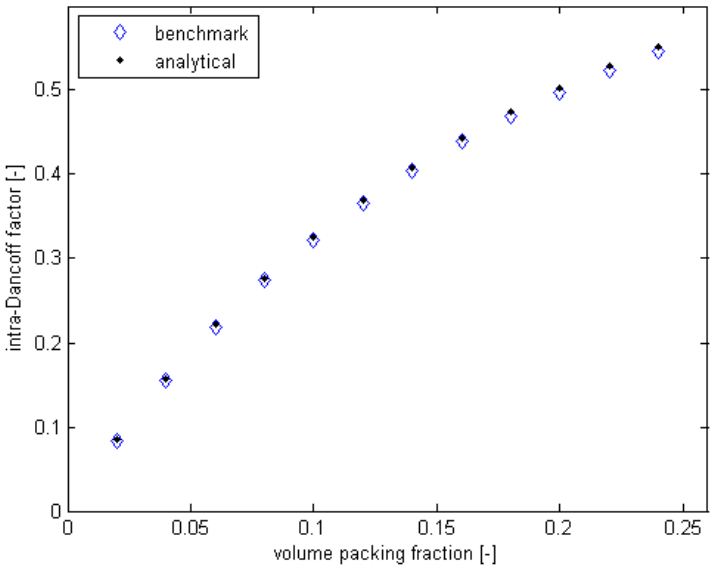

Figure 4.2: C_{intra} analytical results versus benchmark simulation.

also Figure 4.3), which is to be expected since it uses the dual-sphere model. Interestingly, the PDF-LB results seem to slightly underestimate the Dancoff factor for some TRISO packing fractions. This deviation is smaller than that of the analytical results, and is probably related to the accuracy of the histogram algorithm. The average bin path length $\bar{L}$ is calculated as the average of the bin limits, resulting in a slight overestimate of the actual average chord length in the bin. A histogram algorithm that calculates the actual average chord lengths might be able to solve this issue.

4.2 Inter-Dancoff factor

The inter-Dancoff factor can be calculated using Equations 2.18 and 2.19 - 2.22. The calculation of P_1, P_2, P_3 and P_{tr} is very relevant to the accuracy of the inter-Dancoff factor results. The following subsections will present the separate results for these probabilities.

4.2.1 P_1, P_3 and P_{tr}

Because P_1, P_3 and P_{tr} do not depend on $H(S)$, they are not influenced by the pebble shell thickness. This is a very convenient result of the methodology used, because it enables an independent calculation of packing fraction and pebble shell thickness influences on the Dancoff factors and a separate analysis

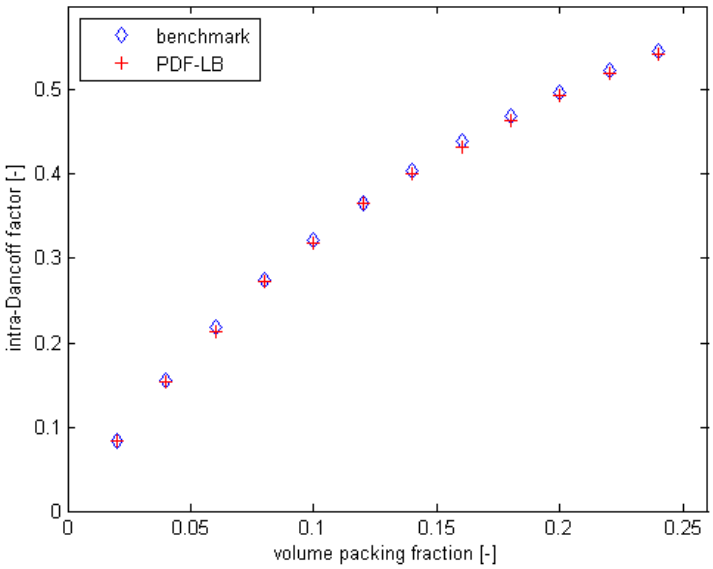

Figure 4.3: C_{intra} results from PDF-LB versus benchmark simulation.

of these influences. Table 4.2 shows the separate probabilities for a range of packing fractions, as calculated using $f(l)$ from PDF-LB.

Packing fraction	P_1	P_3	P_{tr}
0.04	0.41892 ± 0.00017	0.21842 ± 0.00037	0.19453 ± 0.00015
0.08	0.35065 ± 0.00023	0.37145 ± 0.00049	0.13438 ± 0.00019
0.12	0.29849 ± 0.00027	0.48063 ± 0.00057	0.09615 ± 0.00022
0.16	0.26209 ± 0.00029	0.55411 ± 0.00063	0.07220 ± 0.00023
0.20	0.22898 ± 0.00032	0.61669 ± 0.00067	0.05468 ± 0.00025
0.24	0.20358 ± 0.00034	0.66324 ± 0.00071	0.04270 ± 0.00025

Table 4.2: Separate probabilities over a range of packing fractions.

From the table it is evident that the probabilities show the expected behavior. P_1 is equivalent to the first flight escape probability P^*_{esc} and must therefore decrease as packing fraction increases. P_3 is very similar to the intra-Dancoff factor and must resemble its behavior. Figure 4.4 shows a plot of P_3 and the intra-Dancoff factor. The probability that a neutron incident on a pebble enters a fuel lump within that pebble, appears to be significantly higher than the intra-Dancoff factor. This can be explained by the fact that neutrons incident on a pebble are more likely to travel a longer distance through that pebble.

P_{tr} is the probability that a neutron incident on a pebble traverses it without entering a fuel lump. Its behavior should therefore be similar to that of P_1, the

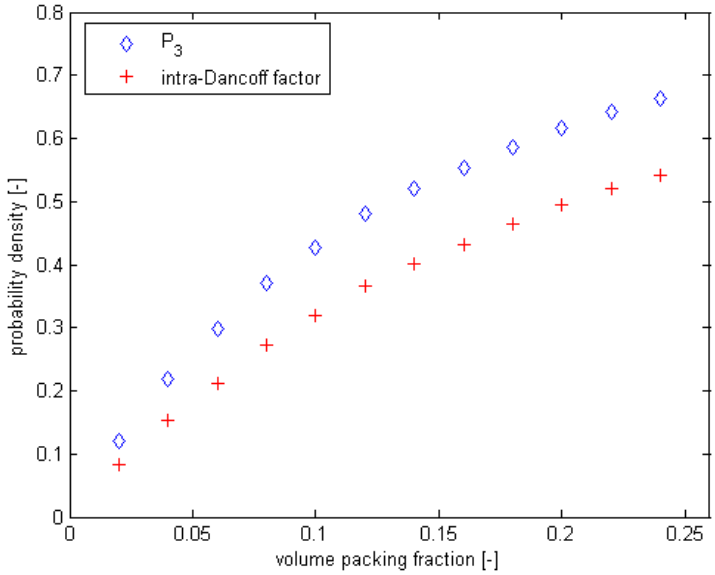

Figure 4.4: P_3 versus intra-Dancoff factor C_{intra}.

first flight escape probability. A plot of these two probabilities over a range of packing fractions is shown in Figure 4.5. P_1 appears to be significantly higher than P_{tr}. Analogous to the explanation for the behavior in Figure 4.4, neutrons originating from a fuel lump inside the pebble are less likely to travel a long distance through the pebble, and therefore are more likely to escape that pebble, as opposed to neutrons that are incident on the pebble.

4.2.2 P_2

P_2 is calculated using either the pebble PDF from PDF-PB, or its analytical approximation by Ji and Martin. The exponential PDF used to approximate $H(S)$ assumed a uniform background moderator. The actual distribution of chord lengths in the pebble bed is a more complicated function, as can be seen in Figure 4.6, which shows a generated PDF (using 1 million neutrons) for the standard pebble size, compared to the analytical PDF.

Since the pebble bed is a closely packed stacking, the pebbles are located at approximately periodic distances from eachother. The first maximum in the plot represents the first 'ring' of pebbles around the initial pebble, and so on. For larger path lengths the rings are less defined, and their associated maxima less distinguishable. This behavior has a strong influence on the calculation of P_2 and therefore a good approximation is required to produce accurate results. Fitting procedures may prove useful to determine a suitable model.

To validate the evaluation of the PDFs from PDF-PB, the results for P_2

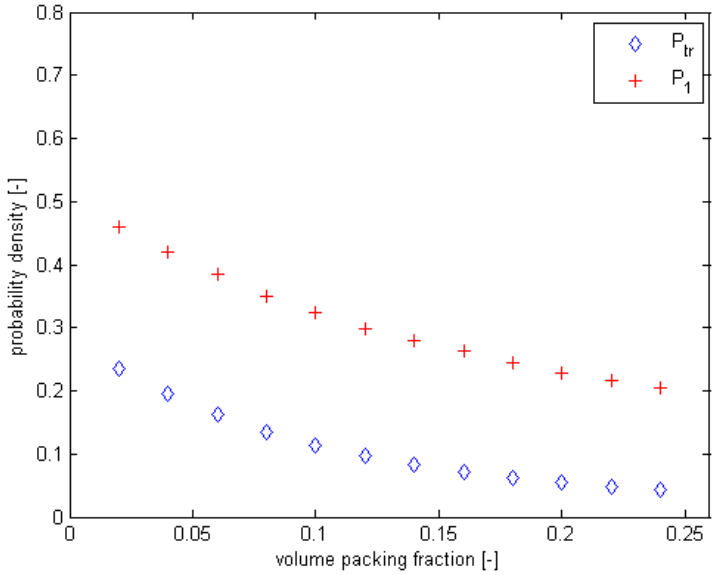

Figure 4.5: P_{tr} versus first flight escape probability P_1.

calculated using those PDFs are shown in table 4.3 versus the benchmark and analytical results by Ji and Martin.

R_{pebble}/R_{fuel}	$P_{2,PDF}$	$P_{2,MC}$	$P_{2,A}$
1.2	0.45887 ± 0.00050	0.4406	0.50188
1.4	0.20979 ± 0.00026	0.1996	0.29606
1.6	0.10095 ± 0.00015	0.0945	0.19154
1.8	0.05048 ± 0.00008	0.0466	0.13179
2.0	0.02614 ± 0.00005	0.0238	0.09485
2.2	0.01387 ± 0.00003	0.0125	0.07065
2.4	0.00755 ± 0.00002	0.0067	0.05410

Table 4.3: P_2 for different pebble shell thicknesses. PDF = results from PDF-PB, MC = Monte Carlo Benchmark, A = analytical results.

From the table it is clear that the PDFs generated by PDF-LB result in a better approximation of P_2 than the function used by Ji and Martin, although not perfect. Because the method used to generate the PDFs is actually a standard Monte Carlo simulation, the deviation might be explained by a difference in simulation method. Another explanation might be that some information is lost when the PDF is generated from the chord lengths, as mentioned in the previous section.

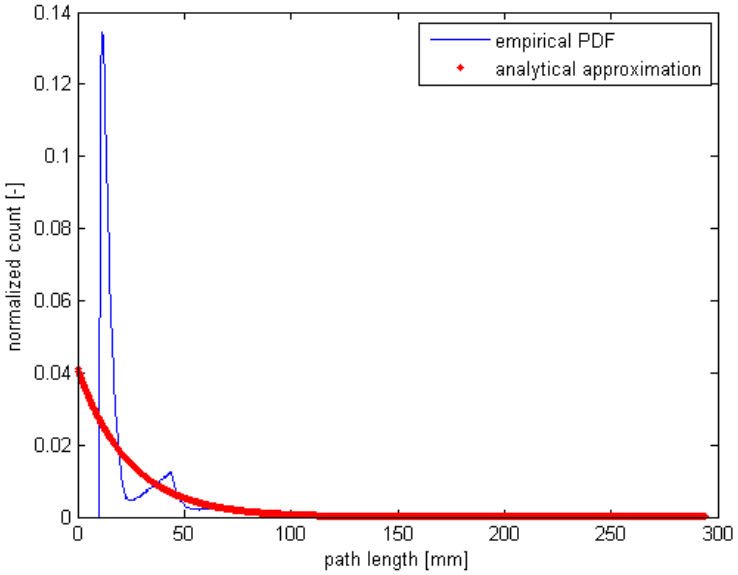

Figure 4.6: Comparison of empirical PDF to analytical approximation of the pebble PDF $H(S)$ for $R_{pebble}/R_{fuel} = 1.2$

4.2.3 C_{inter}

From the separate probabilities the inter-Dancoff factor can be calculated using Equation 2.18. For comparison, C_{inter} was also calculated using the Monte Carlo method by Spoor [16], and using the analytical method by Ji and Martin. The results of these different approaches are shown in Table 4.4, for a range of packing fractions.

Packing fraction	$C_{inter,PDF}$	$C_{inter,MC}$	$C_{inter,A}$
0.04	0.04610± 0.00010	0.04711± 0.00022	0.05287
0.08	0.06369± 0.00012	0.06508± 0.00026	0.07258
0.12	0.06887± 0.00013	0.07041± 0.00027	0.07855
0.16	0.06892± 0.00013	0.07080± 0.00027	0.07858
0.20	0.06646± 0.00014	0.06865± 0.00026	0.07605

Table 4.4: C_{inter} over a range of TRISO packing fractions. PDF = results from PDF-LB and PDF-PB, MC = Monte Carlo Benchmark, A = analytical results.

Interestingly, C_{inter} decreases for higher packing fractions. This is due to the fact that the first flight escape probability decreases with packing fraction, and outweighs the other prabability for higher fractions. Neutrons are less likely to escape the initial pebble at those higher packing fractions.

The errors of the results from PDF-LB and PDF-PB again exceed the uncertainty bounds, with an average error of 2.6%. Although significant, these errors are small compared to the average 11% error by the analytical approach from Ji and Martin. Figure 4.7 shows a plot of these results.

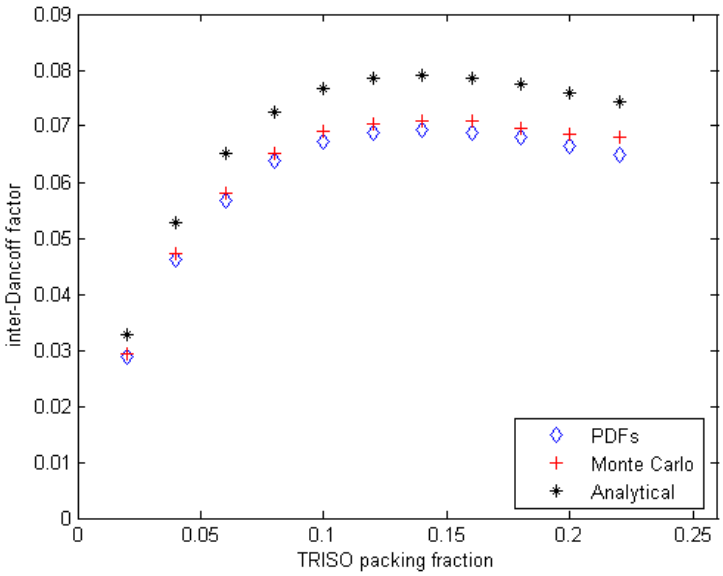

Figure 4.7: PDF, Monte-Carlo, and Analytical calculations of C_{inter} over a range of packing fractions for $R_{pebble}/R_{fuel} = 1.2$.

The analytical description of the fuel zone PDF $H(S)$ causes a significant overestimation of the inter-Dancoff factor. This can be explained in the same way as the deviation found for the intra-Dancoff factor, because the approximation of the PDF leads to a higher hit count for path lengths smaller than the pebble shell thickness.

In order to study the influence of the analytical description of $f(l)$, the inter-Dancoff factor is calculated using the analytical PDF $f(l)$, and the empirical PDF $H(S)$. The results of this semi-analytical approach are shown in Figure 4.8, and surprisingly appear to be a slight improvement compared to the results from the PDF approach with an average error of 1.1%. This means that using analytical description of $f(l)$ leads to an underestimation of C_{inter} through the first flight escape probability P_1. Apparently the underestimation of P_1 compensates for the overestimations of the other probabilities, including that of P_2 by the empirical PDF $H(S)$.

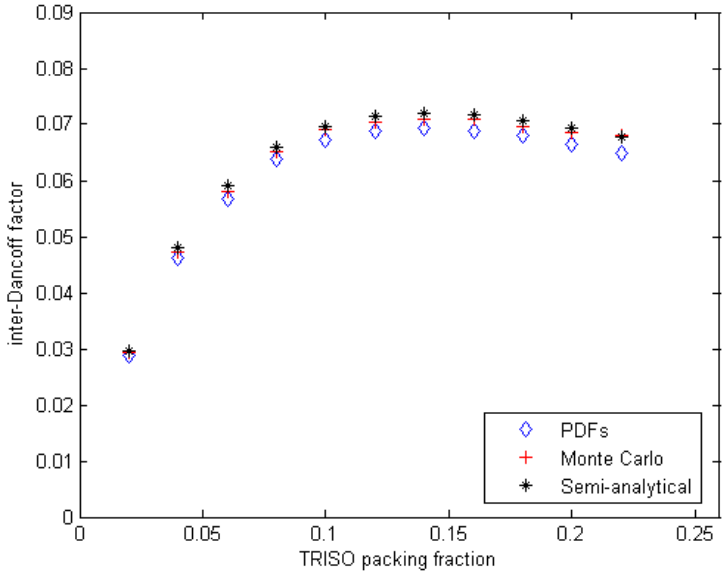

Figure 4.8: PDF, Monte-Carlo, and Semi-analytical calculations of C_{inter} over a range of packing fractions for $R_{pebble}/R_{fuel} = 1.2$.

4.3 Total Dancoff factor

The total Dancoff factor C is the total probability that a neutron escaping from a fuel lump enters another fuel lump before colliding with the moderator. It is given by the sum of the intra- and inter-Dancoff factors $C = C_{intra} + C_{inter}$ and the results of this calculation are presented in Table 4.5, in comparison with the Monte Carlo results using the method of Spoor [16] and the analytical results using that of Ji and Martin [6]. These results are further illustrated in Figure 4.9, which plots C versus the packing fraction.

Packing fraction	C_{PDF}	C_{MC}	C_A
0.04	0.19942± 0.00031	0.20284± 0.00045	0.21029
0.08	0.33584± 0.00042	0.33843± 0.00058	0.34951
0.12	0.43455± 0.00049	0.43586± 0.00066	0.44826
0.16	0.50063± 0.00054	0.50957± 0.00071	0.52181
0.20	0.56033± 0.00059	0.56599± 0.00075	0.57865

Table 4.5: Dancoff factor C over a range of packing fractions. PDF = results from PDF-LB and PDF-PB, MC = Monte Carlo Benchmark, A = analytical results.

The average error of the results compared to the Monte Carlo benchmark

results is 1.1%, the highest error being 2.5%. This is significantly lower than that of the analytical results, with an average of 3% and a highest error of 4.3%. The empirical PDF results show a slight underestimation of the Dancoff factor and the analytical results show an overestimation, both of which can be expected from the results in the previous sections. To investigate the influence of the analytical description of $f(l)$ on the total Dancoff factor, the results are again plotted in Figure 4.10, in comparison to the results calculated using the analytical PDF $f(l)$ and the emprical PDF $H(S)$.

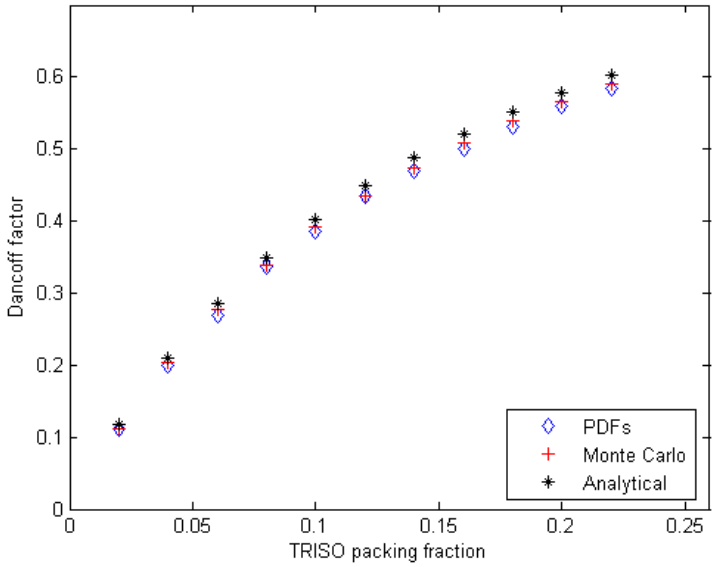

Figure 4.9: PDF, Monte-Carlo, and Analytical calculations of the total Dancoff factor C over a range of packing fractions for $R_{pebble}/R_{fuel} = 1.2$.

This semi-analytical approach proves to be a viable alternative with an average error of 0.5%, and the highest error being 1.2%. Similarly to the semi-analytical calculation of C_{inter}, the slight underestimation of C_{intra} is now compensated by the slight overestimation of C_{inter}.

4.4 Computational method

One of the aims of this research is to investigate whether or not the generation of empirical chord length PDFs is an efficient method for calculating Dancoff factors, as opposed to conventional Monte Carlo simulation or the analytical method by Ji and Martin. Computation time for the generation of the TRISO distributions and their PDFs ranges between 4 and 18 hours, which is compa-

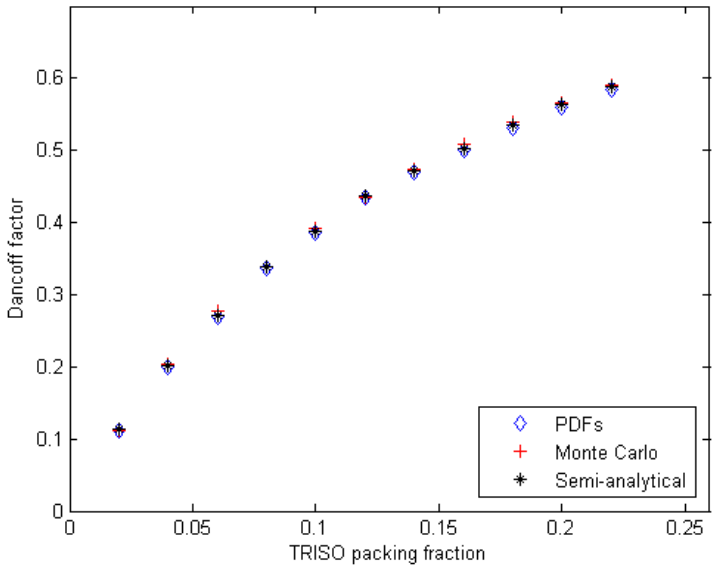

Figure 4.10: PDF, Monte-Carlo, and Semi-nalytical calculations of the total Dancoff factor C over a range of packing fractions for $R_{pebble}/R_{fuel} = 1.2$.

rable to conventional Monte Carlo methods. However, significantly less computation time is required to generate the PDFs from PDF-PB.

The model used fixes some of the problems in the analytical derivations by Ji and Martin. This includes using the dual-sphere model for generating the TRISO PDF, instead of the single sphere-model used by Ji and Martin, which solves the overestimation of the intra-Dancoff factor. Most importantly, a viable PDF is generated to represent the chord lenghts through the moderator between fuel zones. These are two valuable improvements as opposed to the analytical description. The generated PDFs may even be approximated using fitting procedures in order to accomplish a more accurate analytical description of the distributions. More accurate histogram algorithms can be used to improve the accuracy of the generated PDFs.

The main advantage of this methodology lies in its flexibility as opposed to conventional Monte Carlo methods. Instead of generating an entire pebble bed distribution including TRISO coordinates and performing an entire neutron flight path simulation, this method allows for separate generation and analysis of the TRISO and pebble bed PDFs. Once the separate distributions have been generated, they can be combined at will in order to investigate different packing fraction and pebble size combinatins. Furthermore, other complicated VHTR geometries such as the prismatic reactor type might be described using their distribution PDFs.

Chapter 5

Conclusions and recommendations

The central aim of this research was to apply the chord length method derived by Ji and Martin [6] to emprically generated PDFs in order to investigate their model and improve some of the approximations they made. Ji and Martin applied the chord length method to VHTR fuel analysis, and specifically the pebble bed reactor, in order to calculate Dancoff factors. They derived an analytical description of the chord length PDF for distances between TRISO fuel particles using the single sphere model. In order to evaluate the flaws in this approximation, the Fortran code PDF-LB was written, which generated emprical TRISO distribution PDFs using the dual-sphere model, for different volume packing fractions.

Additionally, Ji and Martin did not succeed in deriving a correct model for the distribution of path lengths through the moderator between pebble fuel zones. The Fortran code PDF-PB was written in order to generate empirical PDFs for these chord lengths using a pregenerated pebble stacking.

The generated PDFs were evaluated using a MATLAB script, which calculated the intra- and inter-Dancoff factors for the geometry of interest. The results of these calculations were compared to analytical results using the description by Ji and Martin, and to benchmark results generated using the more standard Monte Carlo method by Spoor [16].

5.1 Conclusions

The PDFs generated by PDF-LB using the dual-sphere model were compared to the analytical description of the PDF by Ji and Martin. The chord length distributions showed substantial differences, especially for smaller chord lengths. The analytical description was predicted to result in a slight overestimate of the intra-Dancoff factor, which was successfully demonstrated. The use of the dual-sphere model in PDF-LB addresses this issue, which resulted in a more accurate

calculation of the intra-Dancoff factor with an average error of 0.1%. The intra-Dancoff factor was calculated over a range of volume packing fractions in the fuel zone, and the expected behavior was demonstrated (as packing fraction increases, so does the intra-Dancoff factor).

PDF-LB was used to generate the PDFs for the distribution of chord lengths between fuel zones in the moderator. These PDFs showed a rather complex behavior because of the nature of the pebble stacking, which explains why the analytical description of this function by Ji and Martin was inaccurate. Several different probabilities that contribute to the inter-Dancoff factor were calculated by evaluating the PDFs from PDF-LB combined with those from PDF-PB using the MATLAB script. The method used to evaluate the PDFs proved to be an effective tool for investigating these different probabilities and their contribution to the inter-Dancoff factor separately. The inter-Dancoff factor was then calculated by combining these probabilities, and compared to the Monte Carlo Benchmark and the analytical results. The results had an average error of 2.6%, which is significant but small compared to the 11% of the analytical results. Another approach involved combining the analytical TRISO distribution PDF with the empirical fuel zone distribution PDF in order to study the influence of the TRISO distribution PDF approximation on the inter-Dancoff factor.

Finally the total Dancoff factor was calculated with an average error of 1.1%, as opposed to 3% by the analytical approach. The semi-analytical approach used to investigate the influence of the TRISO distribution PDF was also used to calculate the Dancoff factor and proved to be a viable alternative with an average error or 0.5%. This means that the analytical TRISO distribution PDF, although proven slightly incorrect, remains a viable resource in calculating Dancoff factors. In combination with an empirical fuel zone PDF, which is generally a more complex function, this approach yields accurate results for relatively short computation times (roughly 2 hours). Monte Carlo methods become increasingly cumbersome for high TRISO packing fractions. In these cases a pregenerated set of TRISO distribution PDFs or a viable analytical description of those PDFs can prove to be a powerful tool.

5.2 Recommendations for future research

The method used for calculation of the Dancoff factors has proven to be very flexible and capable of a separate analysis of the involved probabilities. It can be further improved by using a more accurate algorithm for generating the PDFs, or by deriving a better approximation for the actual TRISO distribution PDF using the PDFs generated by PDF-LB. The latter approach may produce similarly accurate results for the intra-Dancoff factor. Combined with the empirical chord lengths generated by PDF-PB this can prove to be a very fast and flexible method for calculating the overall Dancoff factors in various VHTR configurations.

Bibliography

[1] International Energy Agency, "Key World Energy Statistics 2011", OECD/IEA, Paris, (2011).

[2] International Energy Agency, "World Energy Outlook 2011: Key Graphs", IEA, Paris, (2011).

[3] OECD Nuclear energy Agency, "Generation IV International Forum", *www.gen-4.org*, (2001-present).

[4] European Nuclear Society, "Pebble bed reactor", *http://www.euronuclear.org/info/encyclopedia/p/pebble.htm*, (July 2012).

[5] Tsinghua University Institute of Nuclear and New Energy Technology, "HTR-10", *http://www.tsinghua.edu.cn/publish/ineten/5696/index.html*, (July 2010).

[6] W. Ji and W.R. Martin, "Application of the Chord Method to Obtain Analytical Expressions for Dancoff Factors in Stochastic Media", *Nuclear Science Engineering*, Vol. 169, pp. 19-39 (2011).

[7] S. M. Dancoff and M. Ginsburg, Surface Resonance Absorption in a Close-Packed Lattice, CP-2157, (1962).

[8] P.A.M. Dirac, Approximate Rate of Neutron Multiplication for a Solid of Arbitrary Shape and Uniform Density", Declassified British Report MS-D-5, Part I (1962).

[9] K. M. Case, F. De Hoffmann, and G. Placzek, *Introduction to the Theory of Neutron Diffusion*, Vol. I, pp. 1922 (1953).

[10] R.K. Lane, L.W. Nordheim and J.B. Samson, Resonance Absorption in Materials with Grain Structure, *Nuclear Science Engineering*, Vol. 14, pp. 390-396 (1962).

[11] E.E. Bende, A.H. Hogenbirk, J.L. Kloosterman and H. van Dam, Analytical Calculation of the Average Dancoff Factor for a Fuel Kernel in a Pebble Bed High-Temperature Reactor, *Nuclear Science Engineering*, Vol. 113, pp. 147-162 (1999).

[12] J.L. Kloosterman and A.M. Ougouag, Comparison and Extension of Dancoff Factors for Pebble-Bed-Reactors, *Nuclear Science Engineering*, Vol. 157, pp. 16-29 (2007).

[13] S.H. Kim, H-C Kim, J.K. Kim and J.M. Noh, New strategy on the evaluation of Dancoff factor in a pebble bed reactor using Monte Carlo method, *Nuclear Technology*, Vol. 177, pp. 147-156 (2012).

[14] W. Ji and W.R. Martin, "Determination of Chord Length Distributions in Stochastic Media Composed of Dispersed Microspheres", *Transactions of the American Nuclear Society*, Vol. 96, pp. 467-469 (2007).

[15] University of Tennessee, Knoxville, Nuclear Energy, *http://electron6.phys.utk.edu/phys250/modules/module205/nuclear_energy.htm* (July 2012).

[16] F. Spoor, Monte Carlo and analytical calculations of the Dancoff Factor in Pebble Bed Reactors, specifically for Wallpaper Fuel and Moderator Pebbles, *BSc. Thesis*, Delft University of Technology (2012).

[17] G. Ouwendijk, Analysis of randomly stacked pebble bed reactors using a Monte Carlo neutron transport code with a statistical geometry model, *MSc. Thesis*, Delft University of Technology (2011).

[18] P. E. MacDonald et al., NGNP Preliminary Point Design - Results of the Initial Neutronics and Thermal-Hydraulic Assessments During FY-03, INEEL0EXT-03-00870 Rev. 1, Idaho National Engineering and Environmental Laboratory (2003).

[19] G.J. Auwerda, J.L. Kloosterman, A.J.M. Winkelman, J. Groen and V. van Dijk, Comparison of Experiments and Calculations of Void Fraction Distributions in Randomly Stacked Pebble Beds, *PHYSOR 2010 - Advances in Reactor Physics to Power the Nuclear Renaissance*, Pittsburgh, Pennsylvania, USA, (May 2010)